The Canadian Mineralogist
Vol. 33, pp. 521-535 (1995)

CRYSTALLIZATION AND RE-EQUILIBRATION OF ZONED CHROMITE IN ULTRAMAFIC CUMULATES, VAMMALA Ni-BELT, SOUTHWESTERN FINLAND

PETRI PELTONEN

Geological Survey of Finland, FIN-02150 Espoo, Finland

ABSTRACT

Cotectic proportions of chromite and olivine coprecipitated in tholeiitic island-arc-type magmas that intruded the Svecofennian supracrustal rocks of southwestern Finland during the orogeny. Crystal growth of chromite continued until grains became trapped by olivine, or was terminated because of the appearance of clinopyroxene. From grain to grain, Cr/(Cr + Al) varies between 0.25–0.80, whereas Mg/(Mg + Fe^{2+}) varies only little for any given Cr#. The large Cr# range has been related to the continuous depletion of Cr in the magma due to chromite crystallization, and to concomitant enrichment of magma in Al as a response to assimilation of pelitic sediments and accumulation of olivine. Because fractional crystallization took place in feeder conduits at moderate crustal pressures, the possibility remains that some of the Cr# variation arises from polybaric crystallization of chromite during magma ascent. Almost all chromite grains are zoned toward a more Al-rich rim. Such chemical zonation cannot be explained by any postcumulus or subsolidus mechanism, but is interpreted as initial growth-induced zonation, which produces a grain-scale "memory" of the incremental compositional changes that took place during crystal growth. During subsolidus cooling, the grains of chromite re-equilibrated extensively with enclosing silicates by diffusion-controlled Mg–Fe^{2+} cation exchange. This is not only supported by abnormally low (500–600°C) olivine–spinel blocking temperatures, but also by diffusion profiles preserved in the adjacent olivine. Subsolidus re-equilibration between olivine and spinel proceeded to an unusual extent, indicating a slow cooling rate for the ultramafic cumulates of the Vammala Ni-belt.

Keywords: chromite, cumulates, crystal zoning, fractional crystallization, assimilation, subsolidus re-equilibration, diffusion, Proterozoic, Vammala, Finland.

SOMMAIRE

La chromite et l'olivine ont cristallisé en proportions cotectiques à partir d'un magma tholéiitique typique d'un milieu d'arc insulaire, mis en place dans les roches supracrustales lors de l'orogenèse svécofennienne, dans le sud-ouest de la Finlande. La croissance des cristaux de chromite a progressé jusqu'au point où ils ont été piégés par l'olivine, ou bien jusqu'à la formation du clinopyroxène. D'un grain à l'autre, la valeur de Cr/(Cr + Al) (c'est-à-dire, Cr#) varie entre 0.25 et 0.80, tandis que Mg/(Mg + Fe^{2+}) ne varie que peu pour une valeur de Cr# donnée. On explique l'intervalle important des valeurs de Cr# par un appauvrissement progressif du magma en Cr à cause de la cristallisation de la chromite, et par un enrichissement progressif du magma en Al suite à l'assimilation de sédiments pélitiques et à l'accumulation de l'olivine. Comme la cristallisation fractionnée du magma s'est déroulée dans des conduits nourriciers à une pression crustale modérée, la possibilité existe qu'une partie de la variation en Cr# résulte de la cristallisation polybarique de la chromite au cours de la montée du magma. Presque tous les grains montrent une zonation vers une bordure alumineuse. Une telle zonation en composition ne pourrait résulter de ré-équilibrage post-cumulus ou subsolidus; elle indiquerait plutôt une zonation primaire, qui conserve à l'échelle d'un grain une "mémoire" des changements incrémentiels du magma pendant la croissance des cristaux. Pendant le refroidissement, et donc à un stade subsolidus, les grains de chromite ont réagi à grande échelle avec les silicates qui les englobent, par échange diffusionnel de Mg et de Fe^{2+}. Cette interprétation découle non seulement d'une température de blocage entre olivine et spinelle anormalement faible, de 500 à 600°C, mais aussi de profils de composition préservés dans l'olivine contiguë. Le ré-équilibrage entre olivine et spinelle s'est poursuivi à un stade avancé, indication d'un refroidissement prolongé des cumulats ultramafiques de la ceinture nickelifère de Vammala.

(Traduit par la Rédaction)

Mots-clés: chromite, cumulats, zonation des cristaux, cristallisation fractionnée, assimilation, re-équilibrage subsolidus, diffusion, protérozoïque, Vammala, Finlande.

Introduction

The composition of chromite is strongly dependent upon the composition and oxygen fugacity of the parental magma (Irvine 1965, 1967, Hill & Roeder 1974, Sigurdsson & Schilling 1976, Allan *et al.* 1988, Roeder & Reynolds 1991). These parameters in turn are controlled by the conditions prevailing during partial melting, fractional crystallization, convection and mixing in magma chambers, contamination, liquid immiscibility, and gaseous transfer processes. The effect of the pressure of crystallization is not well constrained, but it may exert some control on the composition of chromite by affecting the partition coefficients (Dick & Bullen 1984) and the order of appearance of minerals (Green *et al.* 1971).

Straightforward deduction of igneous events on the basis of chemical variability of chromite is, however, impeded by the strong tendency for it to re-equilibrate under subsolidus conditions (Irvine 1967, Cameron 1975, Medaris 1975, Wilson 1982, Hatton & von Gruenewaldt 1985, Kimball 1990, Johnson & Prinz 1991, Yang & Seccombe 1993, Roeder 1994). Although in this respect unfortunate, this tendency is also of value in providing an opportunity to evaluate the postmagmatic thermal history of igneous bodies. In addition, a wealth of petrogenetic information pertaining to the igneous, subsolidus, and even tectonic history of the host rock is recorded by the chemical zonation in chromite (*e.g.*, El Goresy *et al.* 1976, Allan *et al.* 1988, Ozawa 1989, Michailidis 1990, Sack & Ghiorso 1991).

This work presents a detailed decription of the mode of occurrence, chemical variability and zonation of chromite from the ultramafic cumulates of the Vammala Ni-belt, southwestern Finland. An attempt is made to remove the overlapping effects of alteration, subsolidus reactions and fractional crystallization, and thus trace out the compositional evolution of this mineral. A considerable amount of data now exists concerning the igneous petrology, subsolidus reactions of silicates, and ore-forming processes in cumulates of the Vammala Ni-belt (Peltonen 1995a, b), which provides a sound background with which to interpret the commonly ambiguous chemical variability of chromite.

Regional Geology and an Outline of Cumulates of the Vammala Ni-Belt

The major geotectonic units of the Fennoscandian (formerly known as Baltic) Shield are the Archean basement (3.1–2.5 Ga) and the early Proterozoic (1.9–1.8 Ga) Svecofennian terrane (Fig. 1, inset). The Svecofennian schists in western and southern Finland are predominantly mica gneisses whose protoliths were graywacke–slate turbidites (Simonen 1980). In addition to the formation of abundant granitic rocks, the culmination of the Svecofennian orogeny was accompanied by less voluminous tholeiitic magmatism, now represented by mafic–ultramafic cumulates thorough the Svecofennian terrane. The Vammala Ni-belt in southwestern Finland is a zone of operating and abandoned Ni–Cu sulfide mines and promising prospects that are associated with bodies of primitive olivine-rich cumulate. These bodies are best described as ultramafic plates, pods, pipes, and lenses that "float" in high- to medium-grade metapelites (Fig. 1). Only minor amounts of gabbroic cumulates occur in the region. Thus these ultramafic cumulates cannot represent the basal units of larger fractionated intrusions. Nor do they represent "Alpine-type" peridotites or the products of ultramafic magmas (*e.g.*, komatiites), but have instead been interpreted (Peltonen 1995b) as the remnants of larger synorogenic conduits for basaltic arc-type magmas. Eventually, these conduits became choked by cumulus crystals and were boudinaged into small lenses and fragments by concomitant tectonic movements, probably even before they were completely solidified.

Petrology of the Cumulates and Related Ni–Cu Deposits

Four representative bodies of ultramafic cumulates from the central part of the Vammala Ni-belt were sampled from drill cores that transect whole bodies (Fig. 1). The Vammala intrusion hosts a low-grade magmatic Ni–Cu deposit that has been exploited since 1978 (Häkli *et al.* 1979), and the Ekojoki intrusion is associated with a subeconomic Ni–Cu–PGE deposit. The Posionlahti and Murto intrusions were chosen as representatives of the cumulate bodies that are devoid of known concentrations of sulfides. The Vammala, Ekojoki, and Posionlahti cumulate bodies are enclosed by high-grade migmatitic metapelites, whereas the country rocks of the Murto intrusion were metamorphosed at a somewhat lower grade and did not undergo partial melting during peak regional metamorphism.

Petrography

All the cumulate bodies sampled consist of ortho- and mesocumulates. Although approximately 75% of the igneous pyroxenes and olivine have been replaced by retrograde amphiboles and pseudomorphic mesh-textured serpentine, respectively, the cumulus textures are well preserved. Olivine, the most common cumulus mineral, usually occurs as euhedral grains up to 3 mm in diameter that have well-preserved grain margins. Usually, olivine is the only cumulus mineral, forming 50–70% of the cumulates. Close to the periphery of the cumulate bodies, the modal content of olivine may drop to 40%, at which point clinopyroxene also appears as a cumulus phase. Clinopyroxene (diopside–augite)

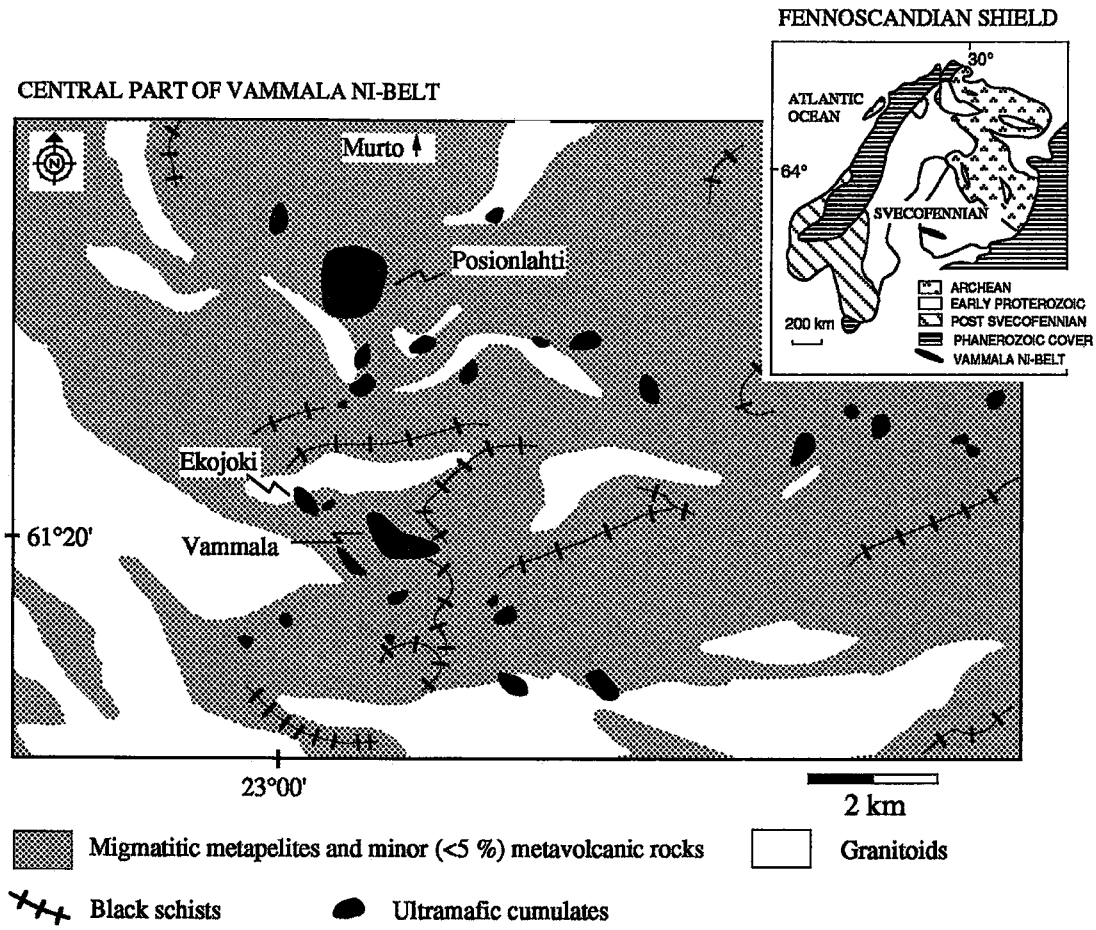

FIG. 1. Simplified geology of the Fennoscandian Shield (inset) and the central part of the Vammala Ni-belt, southwestern Finland.

is the dominant intercumulus mineral, forming oikocrysts up to several centimeters in diameter. Orthopyroxene, which occurs as large oikocrysts and small anhedral grains, is less common than clinopyroxene (cpx:opx ≈ 3:1). Intercumulus amphibole is present only in amounts of a few percent and occurs in the latest intercumulus voids and in a resorption-induced rim around the clinopyroxene; it can generally be distinguished from secondary amphiboles only on the basis of its composition. Most Fe–Ni–Cu sulfides present in the mineralized cumulates occur as interstitial disseminations or as net-textured ore, with pyrrhotite – pentlandite – chalcopyrite ± cubanite ± mackinawite the most common sulfide assemblage.

Petrogenesis

These ultramafic bodies are cumulates derived from a tholeiitic basaltic magma. The order of crystallization was olivine + chromite, followed by clinopyroxene and orthopyroxene, then amphibole. The entry of plagioclase was delayed, probably as a consequence of crystallization at a high confining pressure (*e.g.*, Kushiro & Yoder 1966). Other evidence for crystallization at a moderate to high crustal pressure includes extensive redistribution of Ca between pyroxenes during cooling, high $K_D^{Cpx/Ol}(Mg/Fe)$ values, and the relatively aluminous composition of the pyroxenes. The parental magma that formed these cumulates was pervasively contaminated by local turbidites prior to the final emplacement. Most of the assimilation occurred during ascent of the magma in the arc crust; *in situ* assimilation played only a minor role. Mineral and sulfide compositions of associated magmatic Ni – Cu ± PGE deposits require that sedimentary sulfides participated in ore genesis, and were the ultimate cause for sulfide saturation and segregation in Vammala Ni-belt intrusions (Peltonen 1995a,b).

Four major events, magmatic crystallization, amphibolite-facies prograde metamorphism, retrograde metamorphism, and static serpentinization, are recorded by the mineral assemblages of the cumulates. Owing to their synkinematic emplacement, however, only the outermost margins of the cumulates were susceptible to the prograde growth of minerals, whereas away from the margins, the cumulates largely retained their igneous mineralogy and textures (Peltonen 1995b).

Distribution and Petrography of the Chromite

Euhedral to subhedral grains of chromite are evenly disseminated throughout the cumulates. Its modal abundance does not exceed 2–3% in any sample. Originally, virtually all grains were either included in crystals of cumulus olivine, except for some that were enclosed by intercumulus minerals, or located at grain boundaries between olivine and intercumulus minerals (Fig. 2). In the following discussion, grains in these differing textural settings are referred to as included, intergrain and grain-boundary chromites, respectively (Cameron 1975).

Most grains of chromite are smaller than 50 μm. The average grain-size of grain-boundary and intergrain chromites exceeds that of included grains (Fig. 2). Chromite did not reach saturation much before olivine in the magma, as indicated by the small grain-size (<10 μm) of the chromite in the core of the olivine crystals. The nearly simultaneous saturation of chromite and olivine, followed by their precipitation in cotectic proportions, was not conducive to the formation of chromite-rich cumulus layers. Textural features imply that chromite growth continued until a) grains became trapped by growing crystals of olivine, or b) the appearance of clinopyroxene rapidly consumed the chromium still available.

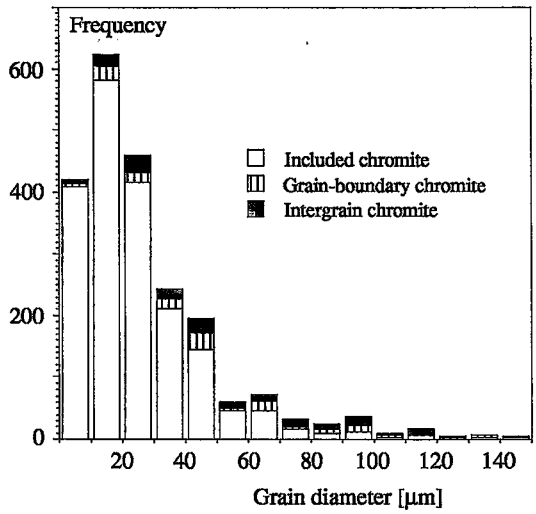

Fig. 2. Grain-size distribution of chromite in the cumulates studied. Note that the relative amount of included chromite is lower in the categories of larger grain-diameter.

Included and intergrain chromites have a well-preserved euhedral to subhedral outline, and are either opaque or almost so, and dark brown in color (Figs. 3A–C). Other morphologies, *e.g.*, skeletal, are completely absent. The reflectance of chromite gradually decreases and the transparency increases outward from the core. Compared to the core area, the rim is lighter brown in transmitted light, and the outermost edge may have a greenish hue. Significantly, those grains completely enclosed by Fe–Ni–Cu sulfides also show similar optical zoning. Some grains of grain-boundary chromite have distinct anhedral protrusions of green spinel that are restricted to the intercumulus side of the crystals (Fig. 3D). Some chromite grains contain tiny inclusions of Fe–Ni sulfide, indicating that immiscible sulfides became saturated in the magma as chromite nucleated. Fractures within chromite grains, related to deformation or serpentinization-related changes in volume, are filled with magnetite, hydrous phyllosilicates and remobilized sulfides.

Locally, zoned grains of chromite are surrounded by an oxidized outer mantle of ferrian chromite, ferrian chromite + magnetite, or magnetite. The reflectance of ferrian chromite is intermediate to that of the chromite and magnetite. Ferrian chromite is most commonly observed around grains of intergrain chromite that are enclosed by secondary amphibole. Where ferrian chromite surrounds chromite grains embedded in lizardite, it may also be associated with chlorite.

Analytical Procedures

From each sample, five to ten grains of chromite of different sizes, and enclosed by various host-minerals, were selected for electron-microprobe analyses. Grain-size measurements were approximated by the diameter of the "best-fit" circle assuming that the plane of the polished thin section passes through the core of the grain, even though in most cases this would be fortuitous. The influence of this sampling effect on results is discussed below. Mineral analyses were done using Cameca SX–50 electron microprobe facilities at the Geoanalytical Laboratory of the Outokumpu Mining Services and at the Geological Survey of Finland. Operating conditions were: 20 kV, 15 nA, beam diameter 5 μm, except for step scans (15 kV, 30 nA, 1 μm). Standards included both synthetic compounds and natural minerals. The peaks were counted for 10–15 seconds, which, for ZnO for example, correspond to a precision of about ± 0.04 wt.%.

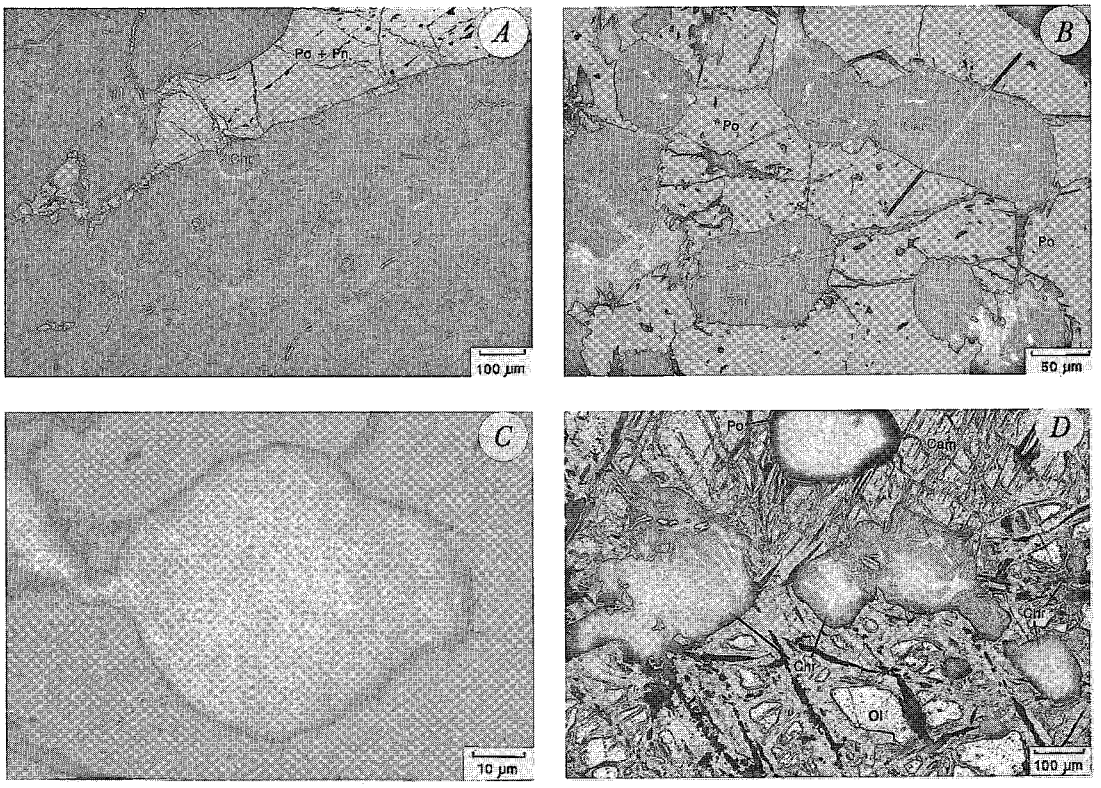

FIG. 3. A. Euhedral to subhedral grains of chromite (Chr) in mineralized olivine–chromite cumulate. Most grains are enclosed by pseudomorphic lizardite (Lz) after primary olivine (Ol), whereas some of the larger grains occupy olivine – intercumulus sulfide (Po + Pn) grain boundaries. B. Intergrain chromite completely enclosed within pyrrhotite. Black line indicates location of the step-scan profile of Fig. 9. C. Included grain of chromite optically zoned toward a rim of higher transparency. D. Large grain-boundary chromite between olivine and calcic clinoamphibole (Cam). Note the green anhedral spinel protrusions along their intercumulus sides.

Total iron was recalculated according to the method of Droop (1987), using stoichiometric criteria. Representative results of the analyses are presented in Table 1.

RESULTS

Chemical variation of the chromite cores

Because the ferric iron content of the cores and rims is uniformly low (Table 1), results can be displayed conveniently in plots of Cr/(Cr + Al) (Cr#) *versus* Mg/(Mg + Fe^{2+}) (Mg#). On the Cr#–Mg# diagram (Fig. 4), the field of the Vammala Ni-belt suite of chromite compositions is distinct from the fields of chromite in Alpine-type and abyssal peridotites (Dick & Bullen 1984), layered intrusions, southeastern Alaskan intrusive bodies (Irvine 1967), and komatiites (*e.g.*, Zhou & Kerrich 1992). Overall, the form and size of the field resemble those of oceanic peridotites and associated lavas (*e.g.*, Dick & Bullen 1984), although the Vammala suite is located at much lower Mg#. Magmatic chromite that has similar Cr#–Mg# systematics to the Vammala Ni-belt suite has only been reported from ultramafic cumulates of island-arc-root complexes (*e.g.*, DeBari & Coleman 1989, Jan & Windley 1990, Kepezhinskas *et al.* 1993).

Several additional fundamental features are displayed by detailed Cr#–Mg# plots (Fig. 5). Such plots indicate that, especially in the case of included grains, a positive correlation exists between Cr# and grain size. Some of this effect arises from the exposure of random sections of zoned grains on the polished surface. However, at least two findings, namely that zoning with respect to Cr# within one grain is much less extensive than variation between samples, and that the smallest grains are indeed visibly euhedral in shape, suggest that this sampling effect is not responsible for

TABLE 1. REPRESENTATIVE[1] RESULTS OF ELECTRON-MICROPROBE ANALYSES OF CHROMITE, VAMMALA Ni-BELT

Code[2]	P1		P27			V59			V61		V70			
Grain location[3]	P		O			SS			O		S			
Diameter [µm]	65		50			150			60		120			
Point location[4]	*core*	*rim*	*core*	*rim*	*fe-chr*	*core*	*rim*	*fe-chr*	*core*	*rim*	*core*	*rim*	*fe-chr*	*mag*
SiO_2 (wt.%)	0.03	0.04	0.01	0.00	0.02	0.00	0.01	0.00	0.00	0.02	0.01	0.04	0.01	0.03
Al_2O_3	12.00	13.27	15.32	16.54	2.98	20.77	23.60	10.99	18.02	18.41	22.32	26.36	11.47	0.01
Fe_2O_3	6.77	7.56	7.36	7.10	26.40	6.89	7.15	16.28	5.93	6.09	7.92	7.64	15.09	69.46
FeO	29.66	29.60	29.60	29.65	30.87	26.70	26.49	29.65	27.53	27.08	26.52	26.24	29.35	31.64
MgO	2.61	2.87	2.61	2.68	0.76	4.61	5.05	2.03	3.93	4.14	4.94	5.63	2.22	0.12
CaO	0.05	0.08	0.03	0.01	0.01	0.02	0.02	0.00	0.02	0.03	0.06	0.02	0.01	0.02
TiO2	0.56	0.63	0.56	0.56	0.88	0.39	0.32	0.34	0.44	0.41	0.31	0.21	0.30	0.00
MnO	0.33	0.37	0.46	0.33	0.44	0.41	0.38	0.58	0.47	0.45	0.47	0.38	0.63	0.00
V_2O_3	0.77	0.79	0.61	0.63	0.79	0.49	0.47	0.55	0.48	0.47	0.49	0.45	0.52	0.03
Cr_2O_3	46.75	44.81	42.82	41.67	36.01	37.83	34.97	38.63	42.16	41.28	35.88	31.96	39.71	1.17
NiO	0.00	0.00	0.00	0.01	0.00	0.00	0.03	0.02	0.00	0.08	0.01	0.04	0.05	0.04
ZnO	0.39	0.40	1.03	1.22	0.37	1.35	1.43	0.39	1.45	1.37	1.35	1.24	0.51	0.01
Total	99.92	100.42	100.41	100.40	99.53	99.46	99.92	99.46	100.43	99.83	100.28	100.21	99.87	102.53
Cations/32 oxygens														
Si	0.009	0.011	0.003	0.001	0.007	0.000	0.002	0.000	0.000	0.006	0.003	0.011	0.002	0.010
Al	3.921	4.284	4.912	5.275	1.042	6.469	7.211	3.654	5.654	5.790	6.842	7.909	3.784	0.004
Fe^{3+}	1.412	1.559	1.508	1.446	5.903	1.369	1.394	3.458	1.189	1.222	1.550	1.463	3.178	15.689
Fe^{2+}	6.875	6.780	6.737	6.708	7.671	5.899	5.744	6.996	6.131	6.045	5.769	5.588	6.872	7.943
Mg	1.079	1.173	1.060	1.080	0.336	1.817	1.950	0.853	1.560	1.648	1.915	2.136	0.926	0.052
Ca	0.015	0.022	0.008	0.004	0.002	0.007	0.005	0.000	0.007	0.008	0.016	0.005	0.003	0.006
Ti	0.117	0.129	0.114	0.113	0.196	0.078	0.062	0.073	0.089	0.082	0.060	0.040	0.064	0.001
Mn	0.076	0.085	0.106	0.074	0.111	0.091	0.085	0.140	0.106	0.103	0.104	0.082	0.150	0.000
V	0.170	0.174	0.132	0.136	0.188	0.104	0.097	0.124	0.102	0.101	0.102	0.092	0.116	0.007
Cr	10.244	9.702	9.213	8.915	8.460	7.902	7.168	8.618	8.877	8.710	7.379	6.434	8.790	0.277
Ni	0.000	0.000	0.000	0.003	0.001	0.000	0.006	0.004	0.000	0.016	0.001	0.008	0.010	0.009
Zn	0.080	0.081	0.207	0.243	0.082	0.264	0.275	0.081	0.285	0.270	0.259	0.232	0.105	0.002
Mg#[5]	0.136	0.147	0.136	0.139	0.042	0.235	0.253	0.109	0.203	0.214	0.249	0.277	0.119	0.007
Cr#	0.723	0.694	0.652	0.628	0.890	0.550	0.499	0.702	0.611	0.601	0.519	0.449	0.699	0.986
YFe^{3+}	0.091	0.100	0.096	0.092	0.383	0.087	0.088	0.220	0.076	0.078	0.098	0.093	0.202	0.982

the bulk of the Cr# variation, and that small grains do not simply represent edges of large zoned grains.

The field of Vammala Ni-belt chromite coincides remarkably with the theoretical isothermal-isobaric isopleths of chromite in equilibrium with olivine of a specific forsterite content. Because coexisting olivine contains 77–83 mol.% Fo, the location of the chromite field far to the right of the theoretical high-temperature Fo_{80} isopleth (Fig. 5) indicates that the chromite and the coexisting olivine do not reflect high-temperature equilibrium (Irvine 1965). There is a weak tendency for smaller grains at any given Cr# to have a lower Mg#. Compositional differences between included and intergrain chromites are small but significant. The field of those intergrain crystals of chromite that are enclosed by silicates (pyroxenes and amphiboles) lies at higher Mg# than the field for included chromite. Intriguingly, grains either completely or partly enclosed by intercumulus sulfides have a Mg# value as low as that of grains included in olivine (Fig. 5).

In most cases, core compositions of grain-boundary chromite plot within the same Cr#–Mg# field as the included chromite. Some of them have anomalously low Cr# or compositional zoning that is strongly polarized toward their intercumulus sides (Fig. 3D). The transition from dark brown cores to bright green anhedral protrusions is accompanied by extreme chemical changes (Fig. 6). These protrusions exhibit a great tendency toward stabilization of the spinel ($MgAl_2O_4$) end-member: levels of Al, Mg, Ni, Zn, and Mg# are higher, whereas levels of Cr, Fe^{3+}, Fe^{2+}, Ti, Mn, V and Cr# are lower in protrusions compared to the cores of the grain-boundary spinel.

If ideal spinel solid-solutions are assumed, the distribution of Mg and Fe^{2+} between coexisting olivine and chromite can be used as a geothermometer (Irvine 1965). Owing to the extensive hydration of olivine, only apparent blocking temperatures of the pair olivine–spinel were obtained. Temperatures, calculated according to the calibration of Fabriès (1979) from the core compositions of included chromite and the mean composition of olivine in the same thin sections, are low (500–600°C) and show a weak dependence on grain size (Fig. 7).

TABLE 1. (CONTINUED)

Code	V71	V75		E81		E83		M123		M126	M131		M147	
Grain location	O	P		O		P		OP		O	O		O	
Diameter [μm]	10	100		40		50		150		40	50		70	
Point location	*core*	*core*	*rim*	*core*	*rim*	*core*	*rim*	*core*	*rim*	*core*	*core*	*rim*	*core*	*rim*
SiO_2 (wt.%)	0.03	0.04	0.04	0.02	0.01	0.03	0.05	0.05	0.04	0.04	0.02	0.05	0.04	0.01
Al_2O_3	25.83	15.37	17.12	15.41	15.65	14.99	15.39	29.89	54.50	22.10	24.45	24.64	20.91	21.49
Fe_2O_3	8.99	5.73	6.26	7.08	7.01	6.48	5.97	4.56	3.08	7.14	5.60	5.68	6.08	5.72
FeO	27.32	26.35	26.16	29.72	29.48	28.59	28.39	25.89	17.56	28.18	26.86	26.79	27.87	27.50
MgO	4.89	4.50	4.93	2.71	2.72	3.27	3.32	6.57	14.01	4.34	5.26	5.13	4.50	4.69
CaO	0.06	0.03	0.08	0.13	0.13	0.04	0.09	0.01	0.01	0.01	0.00	0.03	0.05	0.03
TiO2	0.55	0.32	0.38	0.64	0.66	0.49	0.46	0.15	0.02	0.44	0.31	0.30	0.39	0.40
MnO	0.34	0.43	0.39	0.38	0.32	0.39	0.34	0.18	0.10	0.39	0.30	0.26	0.32	0.32
V_2O_3	0.46	0.51	0.50	0.56	0.58	0.49	0.44	0.20	0.06	0.40	0.29	0.33	0.34	0.36
Cr_2O_3	29.93	45.43	43.35	43.01	42.25	44.41	44.08	31.19	7.74	35.90	35.95	35.04	38.85	38.32
NiO	0.05	0.05	0.02	0.05	0.06	0.00	0.03	0.02	0.05	0.00	0.03	0.05	0.01	0.04
ZnO	1.31	1.01	1.03	0.78	0.86	0.90	0.83	0.59	1.02	0.56	1.05	1.15	0.57	0.56
Total	99.76	99.77	100.26	100.49	99.73	100.08	99.39	99.30	98.19	99.50	100.12	99.45	99.93	99.44
Cations/32 oxygens														
Si	0.007	0.009	0.011	0.005	0.002	0.007	0.013	0.013	0.008	0.010	0.006	0.013	0.009	0.003
Al	7.840	4.887	5.361	4.931	5.037	4.805	4.950	8.833	14.114	6.847	7.413	7.514	6.478	6.660
Fe^{3+}	1.743	1.164	1.252	1.446	1.441	1.326	1.227	0.860	0.509	1.412	1.083	1.106	1.202	1.131
Fe^{2+}	5.884	5.944	5.815	6.749	6.733	6.502	6.480	5.429	3.227	6.195	5.778	5.797	6.126	6.049
Mg	1.879	1.809	1.954	1.095	1.108	1.325	1.350	2.457	4.589	1.702	2.017	1.981	1.764	1.838
Ca	0.016	0.010	0.023	0.039	0.038	0.010	0.025	0.002	0.002	0.004	0.000	0.008	0.014	0.008
Ti	0.107	0.065	0.075	0.130	0.136	0.100	0.094	0.028	0.004	0.087	0.060	0.058	0.078	0.079
Mn	0.075	0.099	0.087	0.087	0.073	0.089	0.078	0.039	0.019	0.088	0.065	0.056	0.072	0.072
V	0.096	0.111	0.107	0.121	0.126	0.106	0.097	0.040	0.010	0.084	0.060	0.068	0.071	0.075
Cr	6.094	9.690	9.107	9.232	9.121	9.548	9.512	6.184	1.344	7.462	7.311	7.170	8.074	7.968
Ni	0.011	0.012	0.004	0.010	0.014	0.000	0.007	0.004	0.009	0.000	0.007	0.010	0.002	0.008
Zn	0.248	0.201	0.203	0.156	0.173	0.181	0.167	0.109	0.165	0.109	0.199	0.219	0.110	0.109
Mg#	0.242	0.233	0.252	0.140	0.141	0.169	0.172	0.312	0.587	0.216	0.259	0.255	0.224	0.233
Cr#	0.437	0.665	0.629	0.652	0.644	0.665	0.658	0.412	0.087	0.521	0.497	0.488	0.555	0.545
YFe^{3+}	0.111	0.074	0.080	0.093	0.092	0.085	0.078	0.054	0.032	0.090	0.069	0.070	0.076	0.072

1) Complete data base is deposited in Geological Survey of Finland *Open File Report #K/31.82/2121/94/2* and is available from the Information Bureau of the Geological Survey of Finland, FIN-02150 Espoo, Finland, or as a 3.5" diskette from the author.

2) P, V, E, M refer to the ultramafic cumulate bodies of Posionlahti, Vammala, Ekojoki and Murto, respectively.

3) O: included chrome spinels (enclosed by olivine); P and S: intergrain chrome spinel enclosed by silicates (mostly pyroxene) or Fe-Ni-Cu sulfides, respectively; OP: grain boundary spinels between olivine and pyroxene (or amphibole); SS: grain boundary chrome spinels between sulfides and silicates.

4) *fe-chr*: ferrian chromite; *mag*: magnetite

5) Mg#=Mg/(Mg+Fe^{2+}); Cr#=Cr/(Cr+Al); YFe^{3+}=Fe^{3+}/(Fe^{3+}+Al+Cr)

Zoning within included and intergrain chromites

Gradual and smooth compositional zoning is ubiquitous in chromite of the Vammala Ni-belt. The absence of complex zoning agrees with petrographic observations that chromite crystallization preceded that of plagioclase (El Goresy *et al.* 1976). In most grains, irrespective of whether they are included or intergrain spinel, Al, Mg, and Mg# increase, whereas Cr, Fe^{2+}, and Cr# decrease from core toward the rim (Figs. 5, 8, 9). In addition, Ti and Mn contents show a weak tendency to decrease, and Fe^{3+}, to increase, whereas no zoning of grains with respect to V and Ni was observed. The decrease in Cr toward grain edges is balanced by a concomitant increase of both Al and Fe^{3+}. However, the increase in Fe^{3+} is insignificant compared to that in Al, suggesting that the strong decrease in Cr content was not caused by a sudden increase of $f(O_2)$. The increasing Mg content toward the rim is balanced by a sympathetic decrease in Fe^{2+}. In some grains, Al and Mg decrease, and either Fe^{2+} or Fe^{3+} or both increase. Such compositional trends are characteristic of alteration to ferrian chromite (below), and presumably these rim compositions are affected by surrounding ferrian chromite or magnetite.

Compositional profiles across chromite–olivine boundaries (Fig. 8) indicate that the olivine also is zoned. The forsterite content of the olivine increases toward the contact, being up to 1.2 mol.% higher adjacent to chromite than away from it. Igneous pyroxenes are commonly uralitized, and attempts to measure zoning in pyroxene were unsuccessful.

Ferrian chromite and magnetite mantles

In several cases (but not all), the chromite grains are surrounded by a mantle of ferrian chromite ± magnetite. Although some of the rim compositions are "transitional", the compositional boundary between chromite and ferrian chromite is commonly sharp. Ferrian chromite has higher Fe^{3+}, Fe^{2+}, Ti, Mn and V, but lower Al, Mg and Zn concentrations than the adjacent chromite. Although the Cr content of ferrian chromite can either fall below or exceed that of

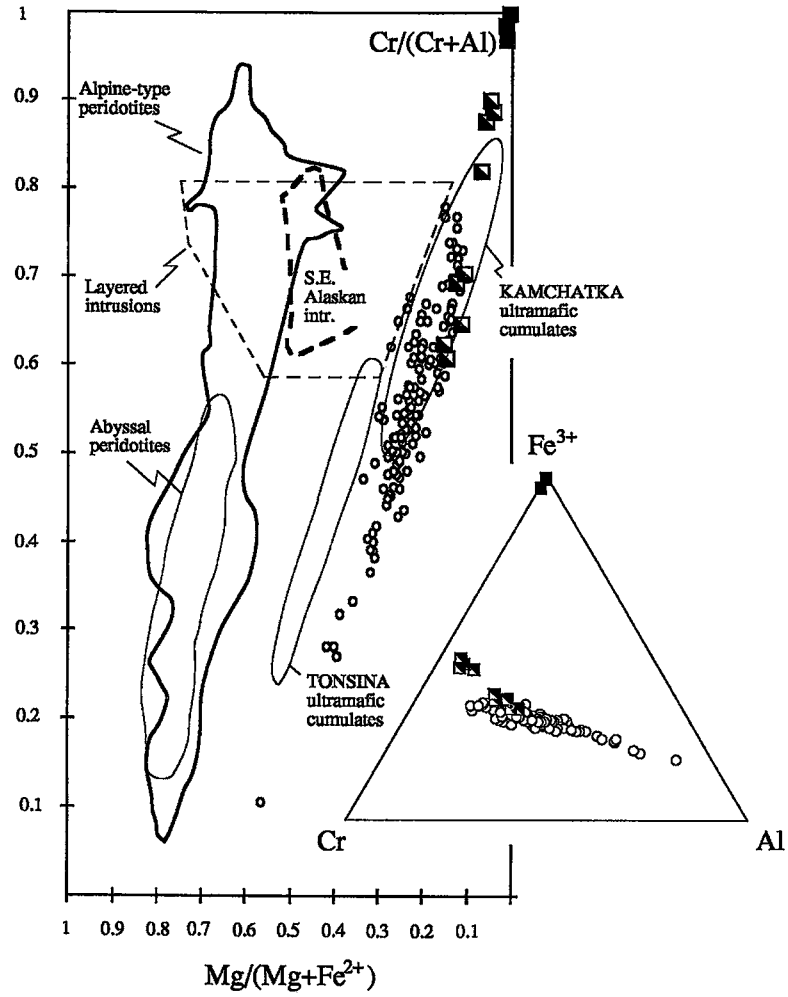

FIG. 4. Compositions of chromite (open circle), ferrian chromite (half-filled square) and magnetite (black square) from the cumulates of the Vammala Ni-belt. Compositional fields of chromite in Alpine and abyssal peridotites (Dick & Bullen 1984), layered and Alaskan-type intrusions (Irvine 1967), and in two island arc root complexes (Tonsina field: DeBari & Coleman 1989, Kamchatka field: Kepezhinskas 1993) are indicated for comparison. The chromite from the Vammala Ni-belt is distinct from chromite reported from komatiites (not shown), which tends to plot within the field of layered intrusions (Zhou & Kerrich 1992).

chromite, the Cr# of ferrian chromite is invariably higher owing to the low Al content of ferrian chromite. Magnetite can be either pure magnetite, nickeloan magnetite or chromian magnetite. Chromite grains that are surrounded by a ferrian chromite ± magnetite mantle have retained their original patterns of Cr–Al and Fe^{2+}–Mg zoning (*e.g.*, P27 and V59 in Table 1).

DISCUSSION

Any satisfactory interpretation of the chemical variation of chromite in these ultramafic cumulates must take the following important observations into account:

(1) The core compositions define an extremely long and narrow field on the Cr# *versus* Mg# diagram, the

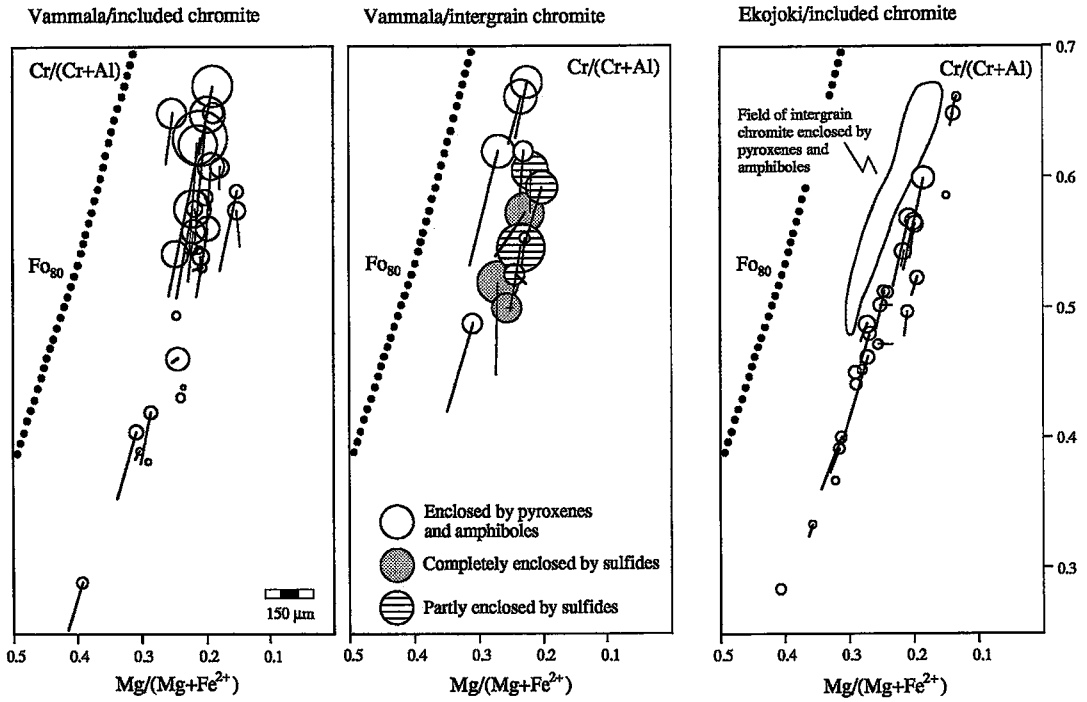

FIG. 5. Detailed Cr#–Mg# plots where core compositions of chromite from Vammala and Ekojoki are represented by circles whose diameters correspond to those of the grains, and where chemical zonation is illustrated by tie lines that connect the core and rim compositions. In these representative cumulate bodies, chromite coexists with olivine that contains 77–83 mol.% Fo. Theoretical Fo_{80} isopleths (after Dick & Bullen 1984) are drawn to semiquantitatively illustrate what the composition of chromite would be if it was in high-temperature equilibrium with adjacent olivine. Scale bar refers to the grain diameter.

slope of this field being close to that of theoretical isothermal-isobaric isopleths of chromite compositions in equilibrium with olivine of a specific Fo content. (2) The chromite grains have an unusually Fe-rich compositions (and a low olivine–spinel blocking temperature) regardless of whether they are included by cumulus olivine, intercumulus silicates or Fe–Ni–Cu sulfides. (3) Intergrain chromite has (at any given Cr# and grain size) a somewhat higher Mg# than included chromite. (4) Practically all grains of chromite are zoned toward a more Al- and Mg-rich rim. (5) The forsterite content of olivine increases toward chromite grains.

Role of metamorphism and alteration

On the Cr#–Mg# plot, the compositional field of the Vammala Ni-belt suite of chromite compositions resembles the field of metamorphic chromite that form in prograde reactions (Evans & Frost 1975, Dymek *et al.* 1988). However, chromite in the cumulates away from the margin of the body is not a member of any prograde metamorphic mineral assemblage, but clearly is an igneous phase, most of which coprecipitated with olivine or immiscible sulfides (Figs. 3A–C). Chromite grains enclosed by pyroxene grains are susceptible to retrograde modifications (*e.g.*, exsolution of spinel during uralitization). However, because all chromite grains, irrespective of whether they are enclosed by minerals like olivine, pyroxenes, sulfides, retrograde amphiboles or serpentine, have the same variation in Cr# and Cr–Al zoning (Figs. 5, 8, 9), regional metamorphism cannot be the fundamental cause for the observed compositional variation. Infrared (IR) spectra and X-ray-diffraction (XRD) studies indicate that the serpentine associated with included chromite is monomineralic lizardite. Pseudomorphic textures considered together with the stability field of lizardite indicate that the hydration of olivine was a static process that occurred at low temperatures and water pressures. Lizardite formation was not followed by reheating, since this would have led to either the replacement of lizardite by non-pseudomorphic antigorite, or metamorphic forsterite + talc ± chlorite (O'Hanley *et al.* 1989). The structure of chromite most

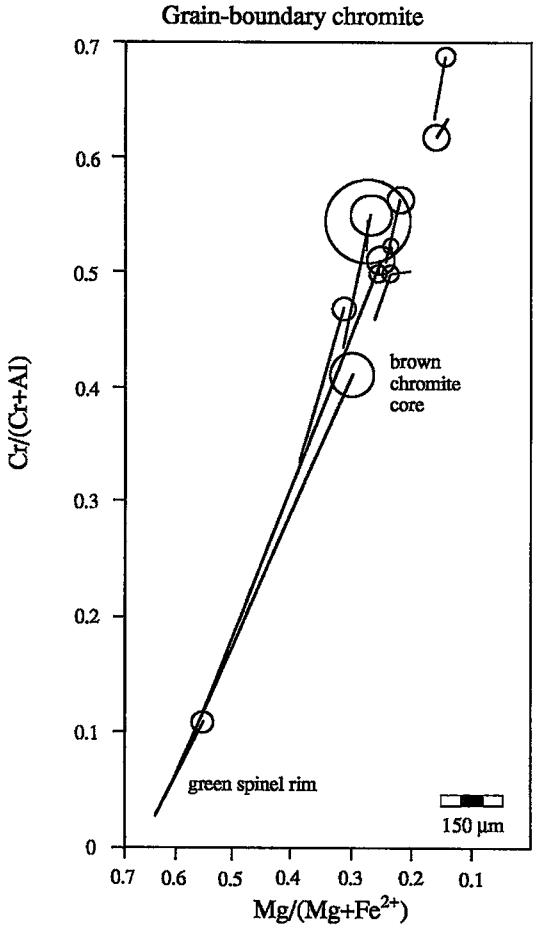

FIG. 6. Cr#–Mg# plot for grain-boundary chromite in the cumulates of the Vammala Ni-belt. Scale bar refers to the grain diameter.

likely is resistant to such static hydration of the enclosing olivine.

Some of the chromite grains are surrounded by a mantle of ferrian chromite. Significantly, the boundary between ferrian chromite and the chromite rim is invariably sharp, and oxidation of iron does not extend deep into the chromite. Since the original description of ferrian chromite material, *i.e.*, "ferritchromit" (Spangenberg 1943), several mechanisms of formation have been proposed (*e.g.*, Beeson & Jackson 1969, Bliss & McLean 1975, Wylie *et al.* 1987, Shen *et al.* 1988, Burkhard 1993). In the cumulates studied here, ferrian chromite occurs between chromite and a) lizardite after olivine, b) secondary amphibole, c) chlorite, and d) magnetite, and apparently has formed by several distinct processes of alteration, detailed analysis of which falls beyond the scope of this contribution. It is worth emphasizing, however, that any reaction involving the formation of ferrian chromite is not a plausible explanation for variable Cr# in the Vammala Ni-belt chromite suite or the ubiquitous Cr–Al zoning, because these features are also invariably present in those grains that are not associated with ferrian chromite.

I conclude that the variability in the Vammala Ni-belt suite of chromite compositions was not generated by metamorphism or alteration, but should be interpreted on the basis of igneous and cooling-related processes.

Origin of grain-boundary chromite

The cores of most grains of grain-boundary chromite have an Mg# as low as that of included chromite, indicating that the extent of chromite–olivine subsolidus re-equilibration does not depend on whether chromite is partly or completely surrounded by olivine. A similar observation was made by Yang & Seccombe (1993), who found that grain-boundary chromite between olivine and plagioclase or between olivine and clinopyroxene re-equilibrated to a similar extent as included grains.

Some of the grain-boundary grains of chromite exhibit asymmetrical anhedral protrusions of green $MgAl_2O_4$-rich spinel toward intercumulus minerals (Fig. 3D). On the basis of textural evidence, these are likely to be a result of postcumulus growth of grain-boundary chromite that was exposed to trapped, extensively fractionated, intercumulus melt. Such growth depletes the adjacent stagnant interstitial liquid in Cr and Fe, causing progressively more Mg- and Al-rich spinel to crystallize (Hamlyn & Keays 1979). Alternatively, the origin of the overgrowths could be attributed to the exsolution of aluminous spinel from pyroxene during cooling or metamorphism. However, because overgrowths are not common around grains of intergrain chromite completely embedded in pyroxene, this is a less satisfactory explanation.

Variation in the Cr# of included and intergrain chromites

Several postcumulus and subsolidus processes are able to change the Cr# of liquidus chromite. Even included chromite is liable to such re-equilibration, because olivine may contain some chromium (Burns 1975, Lehmann 1983, Sutton *et al.* 1993) and aluminum (Jurewicz & Watson 1988, Zhou & Steele 1993), and thus does not act as a perfect barrier to diffusion for these elements. Some investigators have argued that included chromite and intercumulus melt are able to exchange Cr and Al cations through olivine by volume diffusion (Scowen *et al.* 1991), or maintain

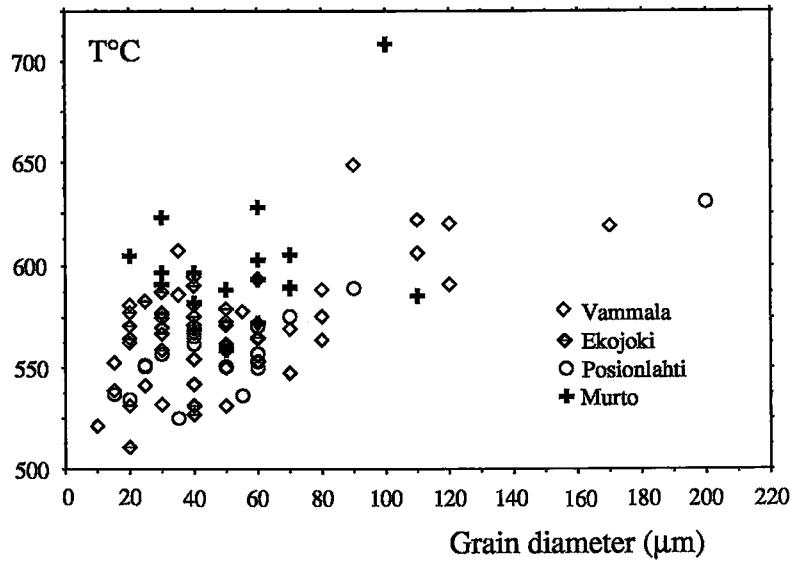

FIG. 7. Variation of olivine–spinel blocking temperature (Fabriès 1979) with the grain size of the included chromite.

contact through fine fractures in olivine (Roeder & Campbell 1985). If volume diffusion through the host mineral were the fundamental cause of the variable Cr# or ubiquitous Cr–Al zoning of chromite in the Vammala Ni-belt cumulates, this would require that diffusion had proceeded exactly to the same extent in olivine, pyroxene and sulfides, which is considered improbable. To be the ultimate cause of the Cr# variation seen in this study, melt-filled fractures, in turn, would have to have penetrated to all grains of included chromite. Furthermore, reaction of included chromite along such fractures with this melt should perhaps have

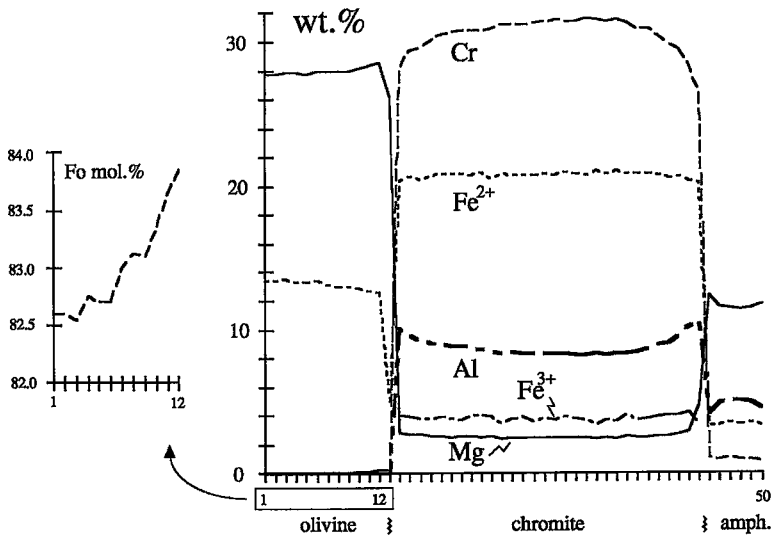

FIG. 8. Step-scan analyses across chromite located between unaltered olivine (left) and Al-rich calcic amphibole (igneous). Length of the profile and individual steps are 180 and 3.6 μm, respectively. Beam diameter was 1 μm.

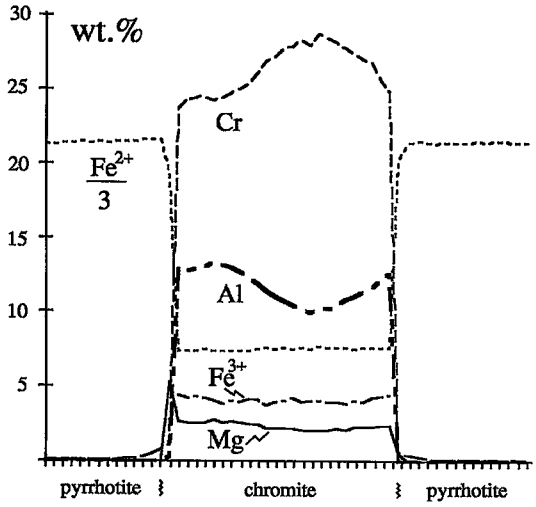

FIG. 9. Step-scan analyses across chromite completely enclosed by pyrrhotite. Length of the profile and individual steps are 190 and 3.2 μm, respectively, with beam diameter of 1 μm. Location of profile is indicated in Fig. 3B.

caused small, needle- or knob-shaped overgrowths, which are not observed.

The solubility of aluminum in pyroxenes is known to decrease as temperature or pressure decreases (*e.g.*, Herzberg 1978, Gasparik & Newton 1984). Cation exchange between chromite and pyroxenes, induced for example by cooling of the intrusions or uplift of the crust, may thus decrease the Cr/Al of intergrain chromite. This probably explains the presence of very aluminous spinel in mantle lherzolites that re-equilibrated at a temperature well below the peridotite solidus (Roeder 1994). The opposite effect, however, is expected for included chromite because the content and diffusivity of Cr in olivine generally exceed those of Al (Jurewicz & Watson 1988, Zhou & Steele 1993). Furthermore, because also those chromite grains completely enclosed by sulfides (which contain some Cr but no Al) have similar patterns of Cr# variation and Cr–Al zoning as are present in included and intergrain chromite, such pressure- or temperature-induced subsolidus processes cannot explain the variable Cr# of chromites in the Vammala suite.

Therefore, I believe that the variable Cr# of included and intergrain chromites should not be interpreted in terms of postcumulus or subsolidus processes, but records evolving magma composition during crystal growth. Some investigators (Sigurdsson & Schilling 1976, Dick & Bullen 1984) have argued that the Cr# of chromite on the liquidus in MORB systems varies inversely with pressure and that highly variable Cr# in such chromite is an expression of its polybaric crystallization. Such an interpretation gains some support from experimental work, which suggests that high confining pressure stabilizes spinel ($MgAl_2O_4$) at the expense of chromite ($FeCr_2O_4$) (Green *et al.* 1971), and from the Al-rich composition of chromite in xenoliths from the mantle (Haggerty 1979) and lower crust (DeBari *et al.* 1987). Because Peltonen (1995b) suggested that cumulates in the Vammala Ni-belt crystallized at mid-crustal pressures, and that the appearance of plagioclase was delayed, the possibility remains that at least some of the variations in Cr# are due to crystallization of chromite under a range of pressure conditions.

Recently, Allan *et al.* (1988) and Roeder & Reynolds (1991) came to the conclusion that melt composition is the only significant variable that controls the composition of chromite at liquidus temperatures, and that a large range in Cr# is an expression of magma mixing or assimilation. There is no evidence for magma mixing in the cumulates of the Vammala Ni-belt. The parental magma of the cumulates was, however, contaminated by Svecofennian graywacke–slate turbidites (Peltonen 1995b). Fractional crystallization under variable pressure conditions, combined with concomitant assimilation of aluminous sediments, were probably the main causes of the large variations in Cr#.

Origin of Cr–Al zoning

Cr–Al-zoned chromite as is found in the Vammala suite is uncommon, but has been reported from the ultramafic Kempirsay intrusion, in the southern Urals (Pustovetov *et al.* 1993), and from a lherzolite nodule found in the Ichinomegata crater, Japan (Ozawa 1983). Unfortunately, these authors do not discuss the origin of the Cr–Al zoning. Lack of details concerning the igneous and metamorphic history of the Kempinsay intrusion, and the nature of the mineral hosting the chromite, prevents further evaluation of that occurrence. In the lherzolite nodule, the chromite is found in aggregates with other Al-bearing phases, pyroxenes and green spinel-bearing symplectite (Ozawa 1983). It is therefore probable that chromite zoning toward an Al-rich rim in the Ichinomegata nodule is due to metamorphic processes. A similar origin for the Cr–Al zoning of chromite in the Vammala Ni-belt is unlikely, because patterns of zoning are equal for all grains, irrespective of whether they are enclosed by magmatic olivine and pyroxenes, their alteration products or sulfides. This zoning must reflect some process that is independent of the identity of the enclosing mineral. One such process is deformation (diffusion creep), which may induce stress-directed self-diffusion of Al and Cr (Ozawa 1989). Deformation-induced zoning is,

however, distinct in the directions of the axes of principal stress. Therefore, Al should, depending on axial orientation, show both increases and decreases toward the rim of randomly oriented grains of chromite, which differs from the observed pattern of Cr–Al zoning.

Finally, one is left with an interpretation that Cr–Al zoning is a grain-scale expression of the same processes that are responsible for the grain-to-grain variation in Cr#. This zoning thus records the incremental compositional changes of the host magma and provides a grain-scale "memory" of the melt evolution during the growth of chromite. Low diffusivities of Cr and Al in chromite, in combination with crystal growth in a vigorously convecting magma, immediately followed by entrapment by olivine, probably prevented further interaction between chromite grains and the magma and preserved the disequilibrium compositions.

Variation in the Mg# of included and intergrain chromite

The fact that the chromite in the Vammala Ni-belt has a considerably more Fe-rich composition than what would coexist with the adjacent olivine at a magmatic temperature (Fig. 5) indicates that the present Mg# of the spinel cores is not purely of igneous origin. Such low Mg# and low olivine–spinel blocking temperatures suggest that the chromite has extensively re-equilibrated with olivine below the solidus. Because the rates of Mg–Fe^{2+} interdiffusion of spinel and olivine are relatively high (Buening & Buseck 1973, Freer & O'Reilly 1980, Wilson 1982, Lehmann 1983), such re-equilibration is a common process in slowly cooled igneous bodies (Irvine 1965, Wilson 1982, Hatton & von Gruenewaldt 1985, Johnson & Prinz 1991, Yang & Seccombe 1993).

That such re-equilibration indeed occurred in the Vammala Ni-belt cumulates is supported by the Mg–Fe^{2+} diffusion profiles for the olivine side of the spinel–olivine grain boundaries (Fig. 8). At the moment the chromite grains were entrapped by olivine, they were in chemical equilibrium. Also at high subsolidus temperatures, disseminated chromite and olivine remain in equilibrium owing to high Mg–Fe^{2+} interdiffusion of both minerals, but at lower temperatures diffusion is unable to maintain Mg–Fe^{2+} equilibrium further, and olivine becomes zoned near the chromite. Lack of complementary Mg–Fe^{2+} diffusion profiles (Fe decreasing toward olivine) in the chromite suggest that Mg–Fe^{2+} interdiffusion in chromite exceeds that in olivine. The extremely narrow range of chromite Mg# (at any given Cr#) reflects the limited compositional range of the olivine with which it re-equilibrated.

Those grains of intergrain chromite that are enclosed by clinopyroxene have systematically rather higher Mg# (and blocking temperatures) than those included in olivine (Fig. 5). Such a finding suggests that Mg–Fe^{2+} interdiffusion in clinopyroxene is lower than that in olivine, but is similar to that in orthopyroxene (Henry & Medaris 1980, Wilson 1982, Hatton & von Gruenewaldt 1985). The low Mg# of intergrain spinel completely enclosed by sulfides is enigmatic (Fig. 5). Overall, composition and zoning are similar to those of other textural types of chromite, indicating that it does not have a distinct origin, and that it also re-equilibrated during the subsolidus stage. Divalent iron is obviously available from the pyrrhotite-dominated sulfides but, because there are no traces of Mg in the sulfide close to chromite (Fig. 9), the sink for Mg^{2+} and specific reactions during the re-equilibration remain unclear.

Conclusions

The composition of chromite grains in the ultramafic cumulates of the Vammala Ni-belt, southwestern Finland, record the evolution of the magma composition during their crystal growth, as well as the thermal conditions during subsequent cooling of the cumulates. This was rendered possible by the distinct diffusional behavior of trivalent (Cr, Al) and divalent cations (Mg, Fe^{2+}) within chromite. The chromite became strongly Cr–Al-zoned because it remained in disequilibrium with the melt that continuously changed its composition owing to fractional crystallization and assimilation. This growth-induced zonation was not modified by subsequent cooling and alteration, implying that the diffusion rates of Cr and Al within chromite must be low. In contrast, the chromite grains were close to ideal Mg–Fe^{2+} exchange equilibrium with the melt and continued to re-equilibrate with enclosing silicates well below the solidus, owing to relatively high Mg–Fe^{2+} interdiffusion in chromite, olivine and pyroxenes, decreasing in this order. The extent to which this re-equilibration proceeded is among the most pervasive so far reported, and is probably a distinct feature of synorogenic mafic–ultramafic intrusions that cooled slowly because of the low temperature-gradient between intrusions and their surroundings.

Acknowledgements

This work was funded by the Geological Survey of Finland (GSF). Dr. K. Korsman (GSF) is thanked for his continuous support of my Ph.D. research, of which this contribution forms a part. Outokumpu Finnmines Ltd. is thanked for providing access to their drill-core repositories, and P. Lamberg (Outokumpu Mining Services) is thanked for running the microprobe and being enthusiastically involved at the earliest stages of this work. This paper benefitted from the thorough reviews of Drs. P. Roeder and P. Scowen, and the editorial comments of Dr. R.F. Martin.

References

ALLAN, J.F, SACK, R.O. & BATIZA, R. (1988): Cr-rich spinels as petrogenetic indicators: MORB-type lavas from the Lamont seamount chain, eastern Pacific. *Am. Mineral.* **73**, 741-753.

BEESON, M.H. & JACKSON, E.D. (1969): Chemical composition of altered chromites from the Stillwater Complex, Montana. *Am. Mineral.* **54**, 1084-1100.

BLISS, N.W & MACLEAN, W.H. (1975): The paragenesis of zoned chromite from central Manitoba. *Geochim. Cosmochim. Acta* **39**, 973-990.

BUENING, D.K. & BUSECK, P.R. (1973): Fe–Mg lattice diffusion in olivine. *J. Geophys. Res.* **78**, 6852-6862.

BURKHARD, D.J.M. (1993): Accessory chromium spinels: their coexistence and alteration in serpentinites. *Geochim. Cosmochim. Acta* **57**, 1297-1306.

BURNS, R.G. (1975): Crystal field effects in chromium and its partitioning in the mantle. *Geochim. Cosmochim. Acta* **39**, 857-864.

CAMERON, E.N. (1975): Postcumulus and subsolidus equilibration of chromite and coexisting silicates in the eastern Bushweld Complex. *Geochim. Cosmochim. Acta* **39**, 1021-1033.

DEBARI, S.M. & COLEMAN, R.G. (1989): Examination of the deep levels of an island arc: evidence from the Tonsina ultramafic–mafic assemblage, Tonsina, Alaska. *J. Geophys. Res.* **94**, 4373-4391.

_____, KAY, S.M. & KAY, R.W. (1987): Ultramafic xenoliths from the Adagdak Volcano, Adak, Aleutian Islands, Alaska: deformed igneous cumulates from the Moho of an island arc. *J. Geol.* **95**, 329-341.

DICK, H.J.B. & BULLEN, T. (1984): Chromian spinel as a petrogenetic indicator in abyssal and alpine-type peridotites and spatially associated lavas. *Contrib. Mineral. Petrol.* **86**, 54-76.

DROOP, G.T.R. (1987): A general equation for estimating Fe^{3+} concentrations in ferromagnesian silicates and oxides from microprobe analyses, using stoichiometric criteria. *Mineral. Mag.* **51**, 431-435.

DYMEK, R.F, BROTHERS, S.C. & SCHIFFRIES, C.M. (1988): Petrogenesis of ultramafic metamorphic rocks from the 3800 Ma Isua supracrustal belt, West Greenland. *J. Petrol.* **29**, 1353-1397.

EL GORESY, A., PRINZ, M. & RAMDOHR, P. (1976): Zoning in spinels as an indicator of crystallization histories of mare basalts. *Proc. 7th Lunar Sci. Conf.*, 1261-1279.

EVANS, B.W. & FROST, B.R. (1975): Chrome-spinel in progressive metamorphism – a preliminary analysis. *Geochim. Cosmochim. Acta* **39**, 959-972.

FABRIÈS, J. (1979): Spinel–olivine geothermometry in peridotites from ultramafic complexes. *Contrib. Mineral. Petrol.* **69**, 329-336.

FREER, R. & O'REILLY, W. (1980): The diffusion coefficient of Fe^{3+} ions in spinels with relevance to the process of maghemitization. *Mineral. Mag.* **43**, 889-899.

GASPARIK, T. & NEWTON, R.C. (1984): The reversed alumina contents of orthopyroxene in equilibrium with spinel and forsterite in the system $MgO–Al_2O_3–SiO_2$. *Contrib. Mineral. Petrol.* **85**, 186-196.

GREEN, D.H., RINGWOOD, A.E., WARE, N.G., HIBBERSON, W.O., MAJOR, A. & KISS, E. (1971): Experimental petrology and petrogenesis of Apollo 12 basalts. *Proc. 2nd Lunar Sci. Conf.*, 601-615.

HAGGERTY, S.E. (1979): Spinels in high pressure regimes. *In* The Mantle Sample: Inclusions in Kimberlite and Other Volcanics (F.R. Boyd & H.O.A. Meyer eds.). *Proc. 2nd Int. Kimberlite Conf.* **2**. American Geophysical Union, Washington D.C. (183-196).

HÄKLI, T.A., VORMISTO, K. & HÄNNINEN, E. (1979): Vammala, a nickel deposit in layered ultramafite, southwest Finland. *Econ. Geol.* **74**, 1166-1182.

HAMLYN, P.R. & KEAYS, R.R. (1979): Origin of chromite compositional variation in the Panton Sill, Western Australia. *Contrib. Mineral. Petrol.* **69**, 75-82.

HATTON, C.J. & VON GRUENEWALDT, G. (1985): Chromite from the Swartkop chrome mine – an estimate of the effects of subsolidus reequilibration. *Econ. Geol.* **80**, 911-924.

HENRY, D.J. & MEDARIS, L.G., JR. (1980): Application of pyroxene and olivine–spinel geothermometers to spinel peridotites in southwestern Oregon. *Am. J. Sci.* **280-A**, 211-231.

HERZBERG, C.T. (1978): Pyroxene geothermometry and geobarometry: experimental and thermodynamic evaluation of some subsolidus phase relations involving pyroxenes in the system $CaO–MgO–Al_2O_3–SiO_2$. *Geochim. Cosmochim. Acta* **42**, 945-957.

HILL, R. & ROEDER, P. (1974): The crystallization of spinel from basaltic liquid as a function of oxygen fugacity. *J. Geol.* **82**, 709-729.

IRVINE, T.N. (1965): Chromian spinel as a petrogenetic indicator. 1. Theory. *Can. J. Earth Sci.* **2**, 648-672.

_____ (1967): Chromian spinel as a petrogenetic indicator. 2. Petrologic applications. *Can. J. Earth Sci.* **4**, 71-103.

JAN, M.Q. & WINDLEY, B.F. (1990): Chromian spinel – silicate chemistry in ultramafic rocks of the Jijal complex, northwest Pakistan. *J. Petrol.* **31**, 667-715.

JOHNSON, C.A. & PRINZ, M. (1991): Chromite and olivine in type II chondrules in carbonaceous and ordinary chondrites: implications for thermal histories and group differences. *Geochim. Cosmochim. Acta* **55**, 893-904.

JUREWICZ, A.J.G. & WATSON, E.B. (1988): Cations in olivine. 2. Diffusion in olivine xenocrysts, with applications to petrology and mineral physics. *Contrib. Mineral. Petrol.* **99**, 186-201.

KEPEZHINSKAS, P.K., TAYLOR, R.N. & TANAKA, H. (1993): Geochemistry of plutonic spinels from the North Kamchatka Arc: comparison with spinels from other tectonic settings. *Mineral. Mag.* **57**, 575-589.

KIMBALL, K.L. (1990): Effects of hydrothermal alteration on the compositions of chromian spinels. *Contrib. Mineral. Petrol.* **105**, 337-346.

KUSHIRO, I. & YODER, H.S., JR. (1966): Anorthite–forsterite and anorthite–enstatite reactions and their bearing on the basalt–eclogite transformation. *J. Petrol.* **7**, 337-362.

LEHMANN, J. (1983): Diffusion between olivine and spinel: application to geothermometry. *Earth Planet. Sci. Lett.* **64**, 123-138.

MEDARIS, L.G., JR. (1975): Coexisting spinel and silicates in alpine peridotites of the granulite facies. *Geochim. Cosmochim. Acta* **39**, 947-958.

MICHAILIDIS, K.M. (1990): Zoned chromites with high Mn-contents in the Fe–Ni–Cr-laterite ore deposits from the Edessa area in northern Greece. *Mineral. Deposita* **25**, 190-197.

O'HANLEY, D.S., CHERNOSKY, J.V., JR. & WICKS, F.J. (1989): The stability of lizardite and chrysotile. *Can. Mineral.* **27**, 483-493.

OZAWA, K. (1983): Evaluation of olivine–spinel geothermometry as an indicator of thermal history for peridotites. *Contrib. Mineral. Petrol.* **82**, 52-65.

_____ (1989): Stress-induced Al–Cr zoning of spinel in deformed peridotites. *Nature* **338**, 141-144.

PELTONEN, P. (1995a): Magma – country rock interaction and the genesis of Ni–Cu deposits in the Vammala Nickel Belt, SW Finland. *Mineral. Petrol.* **52**, 1-24.

_____ (1995b): Petrogenesis of ultramafic rocks in the Vammala Nickel Belt: implications for crustal evolution of the early Proterozoic Svecofennian arc terrane. *Lithos* **34**, 253-274.

PUSTOVETOV, A.A., MITINA, YE.A., UKHANOV, A.V., NIKOL'SKAYA, N.YE. & SENIN, V.G. (1993): Inhomogeneity in accessory chrome spinel as a geothermometer. *Geochem. Int.* **30**(5), 31-41.

ROEDER, P.L. (1994): Chromite: from the fiery rain of chondrules to the Kilauea Iki lava lake. *Can. Mineral.* **32**, 729-746.

_____ & CAMPBELL, I.H. (1985): The effect of post-cumulus reactions on composition of chrome-spinels from the Jimberlana intrusion. *J. Petrol.* **26**, 763-786.

_____ & REYNOLDS, I. (1991): Crystallization of chromite and chromium solubility in basaltic melts. *J. Petrol.* **32**, 909-934.

SACK, R.O. & GHIORSO, M.S. (1991): Chromite as a petrogenetic indicator. *In* Oxide Minerals (D.H. Lindsley, ed.). *Rev. Mineral.* **25**, 323-353.

SCOWEN, P.A.H., ROEDER, P.L. & HELZ, R.T. (1991): Reequilibration of chromite within Kilauea Iki lava lake, Hawaii. *Contrib. Mineral. Petrol.* **107**, 8-20.

SHEN, PUYAN, HWANG, SHYH-LUNG, CHU, HAO-TSU & JENG, RUEY-CHANG (1988): STEM study of "ferritchromit" from the Heng-Chun chromitite. *Am. Mineral.* **73**, 383-388.

SIGURDSSON, H. & SCHILLING, J.-G. (1976): Spinels in Mid-Atlantic Ridge basalts: chemistry and occurrence. *Earth Planet. Sci. Lett.* **29**, 7-20.

SIMONEN, A. (1980): The Precambrian of Finland. *Geol. Surv. Finland Bull.* **304**.

SPANGENBERG, K. (1943): Die Chromerzlagerstätte von Tampadel am Zobten. *Z. Prakt. Geol.* **51**, 13-35.

SUTTON, S.R., JONES, K.W., GORDON, B., RIVERS, M.L., BAJT, S. & SMITH, J.V. (1993): Reduced chromium in olivine grains from lunar basalt 15555: X-ray absorption near edge structure (XANES). *Geochim. Cosmochim. Acta* **57**, 461-468.

WILSON, A.H. (1982): The geology of the Great "Dyke", Zimbabwe: the ultramafic rocks. *J. Petrol.* **23**, 240-292.

WYLIE, A.G., CANDELA, P.A. & BURKE, T.M. (1987): Compositional zoning in unusual Zn-rich chromite from the Sykesville district of Maryland and its bearing on the origin of "ferritchromit". *Am. Mineral.* **72**, 413-422.

YANG, KAI & SECCOMBE, P.K. (1993): Chemical variation of chromite in the ultramafic cumulates of the Great Serpentinite belt, Upper Bingara to Doonba, New South Wales, Australia. *Can. Mineral.* **31**, 75-87.

ZHOU, MEI-FU & KERRICH, R. (1992): Morphology and composition of chromite in komatiites from the Belingwe Greenstone Belt, Zimbabwe. *Can. Mineral.* **30**, 303-317.

ZHOU, Y. & STEELE, I.M. (1993): Chemical zoning and diffusion of Ca, Al, Mn, and Cr in olivine of Springwater pallasite. *Proc. 24th Lunar Sci. Conf.*, 1573-1574.

Received April 6, 1994, revised manuscript accepted September 20, 1994.